Effects of lanthanum doping on the dielectric properties of $Ba(Fe_{0.5}Nb_{0.5})O_3$ ceramic

Chao-Yu Chung and Yen-Hwei Chang[a)]
Department of Material Science and Engineering, National Cheng Kung University, Tainan 701, Taiwan, Republic of China

Guo-Ju Chen
Department of Material Science and Engineering, I-Shou University, Kaohsiung 840, Taiwan, Republic of China

(Received 1 December 2003; accepted 16 August 2004)

The relaxor type of ferroelectric material $Ba(FeNb)_{1/2}O_3$, which has a partially disordered perovskite structure, has been characterized and shown a maximum plateau of the dielectric permittivity depending upon the temperature. The dielectric constant at a low frequency is up to 30 000 at room temperature. While the single-phase La-doped $Ba(FeNb)_{1/2}O_3$, $Ba_{1-x}La_x(Fe_{1/2}Nb_{1/2})_{1-x/4}O_3 (0 \leqslant x \leqslant 0.2)$ has a monoclinic structure solid solutions up to $x \leqslant 0.2$, the lattice parameters decrease with an increasing La concentration. The temperature dependence of the dielectric constant of the La-doped $Ba(FeNb)_{1/2}O_3$ was measured with different La contents, showing that the dielectric permittivity is higher than 10^5 at an 8 mol% La concentration. The present dielectric dispersion was interpreted on the basis of the interfacial polarization at the grain-boundary region. © *2004 American Institute of Physics*. [DOI: 10.1063/1.1804243]

I. INTRODUCTION

Oxides with perovskite structures and high dielectric constants play an important role in microelectronics, and have numerous technological applications. They have been used as memory devices and capacitors. Dielectric materials always exhibit with ferroelectric or relaxor properties. However, both kinds of materials have dielectric constants that vary hugely with temperature, a property which is unfavorable for many applications. However, most perovskite structure dielectric materials contain lead, but the environment is polluted by lead. Therefore, lead-free materials with high dielectric constants are becoming increasingly attractive.

A lead-free perovskite-like oxide, $CaCu_3Ti_4O_{12}$[1,2] was recently reported to have an extraordinarily high static dielectric constant of $\varepsilon_0 \approx 10^5$ at room temperature. Furthermore, while Li and Ti-doped NiO is a new oxide with a high dielectric constant,[3] it does not have a perovskite structure and it is not non ferroelectric, but it does have a low-frequency dielectric constant of $\varepsilon_0 \approx 10^4 - 10^5$ at room temperature. $Ba(FeNb)_{1/2}O_3$ is a relaxor type of ferroelectric material that has a partially disordered perovskite structure.[4,5] Its curve of dielectric permittivity versus temperature includes a plateau after the maximum. These relaxor ferroelectric properties follow from the broad dielectric transitions, known as the diffused phase transitions with a strong frequency dispersion.[6,7]

This investigation examines the effects of La doping on the $Ba(FeNb)_{1/2}O_3$ samples prepared according to the formula $Ba_{1-x}La_x(Fe_{0.5}Nb_{0.5})_{1-x/4}O_3 (0 < x < 0.2)$. The charges of the La ion were compensated by the appearance of the *B*-site vacancies. Incorporating La_2O_3 into the *A*-site sublattice of the perovskite structure stabilizes in the monoclinic phase, and the polycrystalline materials of such modified dielectrics were prepared by a solid-state reaction method. The microstructures and the corresponding dielectric properties were characterized.

II. EXPERIMENT

The compounds used in this investigation were prepared by a routine solid-state reaction route and starting materials, which included $BaCO_3$ (99.9% pure, NOAH technologies corporation, San Antonio), Fe_2O_3 (99.9% pure, Alfa Asear Co.), Nb_2O_5 (99.9% pure, Aldrich Chemical Co.), and La_2O_3 (99.99% pure, Showa Chemical Co., Ltd.). The donor (La) doping concentration were varied from 0.02 to 0.2 mol% and the raw powders were based on the formula $Ba_{1-x}La_x(Fe_{0.5}Nb_{0.5})_{1-x/4}O_3$. The columbite precursor method was used for the $FeNbO_4$ powders, first synthesized by prereacting the Fe_2O_3 and Nb_2O_5 ball milled with acetone in a polypropylene jar for 24 h. The mixture was then dried at 100 °C and calcined at 1100 °C for 4 h in air. Secondly, the $Ba_{1-x}La_x(Fe_{0.5}Nb_{0.5})_{1-x/4}O_3$ powders were prepared by the $FeNbO_4$, $BaCO_3$, and La_2O_3 ball milled with acetone in a polypropylene jar for 24 h again, and after drying, they were calcined at 950 °C for 5 h in air. 1 wt% of polyvinyl alcohol was usually added to the synthesized powders as the sintering aid. The calcined powders were regrounded and pressed at 200 MPa in the form of disks of 10–11 mm in diameter and thicknesses of 2–4 mm. Finally, the pellets placed on an aluminum oxide crucible were sintered in air at 1200–1350 °C for 4 h at a ramping rate of 5 °C/min. The electrodes for measurements were deposited on grinded disk surfaces by rubbing on the In–Ga alloy.

The phase purity, the structure, and the lattice parameters of the sample were determined by x-ray power diffraction

[a)]Author to whom correspondence should be addressed; electronic mail: enphei@mail.ncku.edu.tw

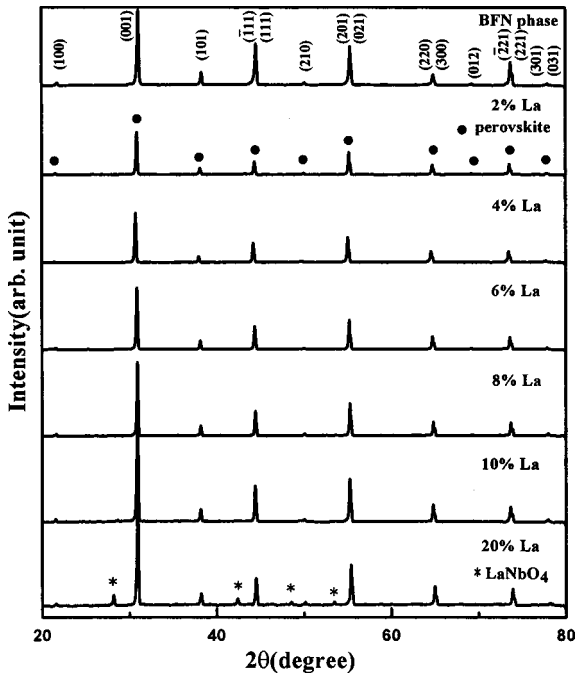

FIG. 1. XRD patterns of $Ba_{1-x}La_x(Fe_{0.5}Nb_{0.5})_{1-x/4}O_3$ ceramics with various x values, sintered at 1350 °C for 4 h.

with Cu$K\alpha$ radiation at room temperature. The particle morphology and the grain size were characterized by scanning electron microscopy (SEM). The density of sintered $Ba_{1-x}La_x(Fe_{0.5}Nb_{0.5})_{1-x/4}O_3$ was measured using the Archimedes method in de-ionized water. The dielectric constant and dielectric loss were measured from 100 Hz to 100 kHz at room temperature using an LCR (HP4284A) meter.

III. RESULT AND DISCUSSION

A. Crystal structure, density, and microstructure

Figure 1 shows the x-ray diffraction (XRD) patterns (at room temperature) of the sintered ceramics with formula $Ba_{1-x}La_x(Fe_{0.5}Nb_{0.5})_{1-x/4}O_3$ and various x values. All the reflection peaks of the x-ray profile were indexed and the lattice parameters were determined using the least-square method with the help of a standard computer program. The results show that the compound with $x=0$ has a monoclinic structure at room temperature with $\beta=90.165°$. Furthermore, the x-ray diffraction confirms that the specimen is a single phase for x of up to 10%. However, the extensive substitution at $x=20\%$ generated the $LaNbO_4$ secondary phase. The lattice constants were determined from their diffraction patterns using the computer program Unit Cell. The lattice parameters decreased as the La content increased, because $La^{3+}(1.32A^0)$ has a smaller ionic radius than $Ba^{2+}(1.60A^0)$.[8,9] The cell volume decreases slightly and the beta angle approaches 90° as La increases (Table I).

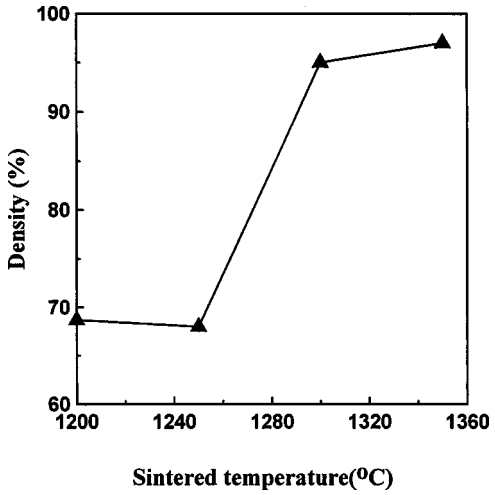

FIG. 2. Relationship between the density and the sintering temperature for 2% La-doped BFN.

Figure 2 shows the variation of sintering density as a function of temperature for $Ba_{0.98}La_{0.02}(Fe_{0.5}Nb_{0.5})_{1-0.02/4}O_3$. The sintering density rises sharply as the temperature is raised from 1250 to 1350 °C to achieve the maximum of ~97% theoretical density. Increasing the sintering temperature enhances the growth of grains and reduces the porosity. Additionally, Fig. 3 shows that when the sintered temperature is 1350 °C, the density of the entire sample will be higher than 95%. Figure 4 displays the SEM photographs of the BFN with x% La sintered at 1350 °C for 4 h. The average grain size was found to decrease as the La content increased, because the doping trivalent-ion La^{3+} (1.32 Å) in BFN occupied Ba sites, favoring the formation of donor imperfections $Ba_{La}^{\cdot}$. However, these ions can also occupy the Fe sites or Nb site and thus act as acceptors. This leads predominantly to electric and barium vacancy compensation in the undoped BFN and at a low doping level.[10,11] As the doping concentration is increased, either self-compensation or B-site vacancy compensation becomes more pronounced at the ex-

TABLE I. Structure, lattice parameters, unit-cell volumes, and average grain sizes for various compositions (x) in the system of $Ba_{1-x}La_x(Fe_{0.5}Nb_{0.5})_{1-x/4}O_3$.

	Lattice parameters					
Composition (x)	a(Å)	b(Å)	c(Å)	Structure	Bata	Unit-Cell volume ($x10^{-30}$ m^3)
0%	4.0717	4.0525	2.8763	monoclinic	90.165	47.4596
2%	4.0736	4.0485	2.8789	monoclinic	90.255	47.4773
4%	4.0629	4.0498	2.8709	monoclinic	90.108	47.2384
6%	4.0640	4.0540	2.8748	monoclinic	90.097	47.3637
8%	4.0574	4.0452	2.8677	monoclinic	90.053	47.0665
10%	4.0537	4.0472	2.8655	monoclinic	90.034	46.9841
20%	4.0455	4.0380	2.8600	monoclinic	90.024	46.7208

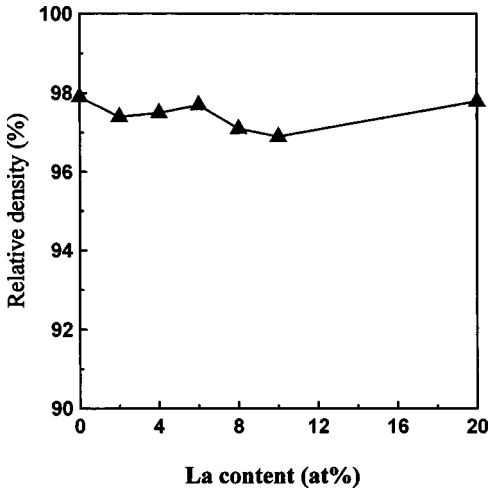

FIG. 3. The variation of density with La-doped leave. Ceramic sintered at 1350 °C for 4 h.

pense of electron compensation. Both mechanisms may also operate simultaneously.[12,13] Additionally, at a high level of doping, additional vacancy pairs in the form of $V_O^{\cdot\cdot}-V_{Ti}^{''''}$ can also be expected to compensate for oxygen vacancies ($V_O^{\cdot\cdot}$). On the other hand, grain boundaries also enhance the influence on the trapping property of positrons.[13,14] As x increases from 0% to 10%, the grain size decreases from 10 to 3 μm, as shown in Figs. 4(a)–4(c), that there is a critical value of a doped concentration (1 mol% La) at which the grain size has the tendency to grow, and it shows that almost all the grains exhibit a clear and a similar core-shell structure, as shown in Fig. 4(d). The contrast between the grains and the grain boundaries represents different compositional distribution. This result explained that La-doped concentration is more than 10 mol%, the secondary phase $LaNbO_4$, which is easily segregated into the grain boundary, will influence the dielectric constant.

B. Dielectric behavior

Figures 5(a) and 5(b) plot the relationship between the dielectric constants and the sintering temperatures and the La concentration at room temperature, respectively, as measured at a frequency of 1 kHz. The dielectric constants increase with the sintering temperature and the sintered density, because the density improvement reduces the porosity. Figure 5(b) reveals that increasing the doping level induces many compensation mechanisms, such as electric compensation, *B*-site vacancy compensation, and oxide vacancy compensation, all of which cause a strong polarization.

The temperature dependence of the relative dielectric constant and dissipation factor (D) of $Ba(FeNb)_{1/2}O_3$: x% La versus temperature is shown in Fig. 6. The dielectric constants increase with the increasing La concentration over a wide range of temperatures from 298 to 440 K. When the La concentration is at 8 mol%, the dielectric constant (at 1 kHz) is greater than 10^5, as measured at 370 K and above. The dissipation factor (D) depends weakly on temperature. The dielectric constant at a La concentration of 20 mol% is lower than at a La concentration of 8 mol%, as measured at 420 K and above. This effect is related to the presence of the second phase.

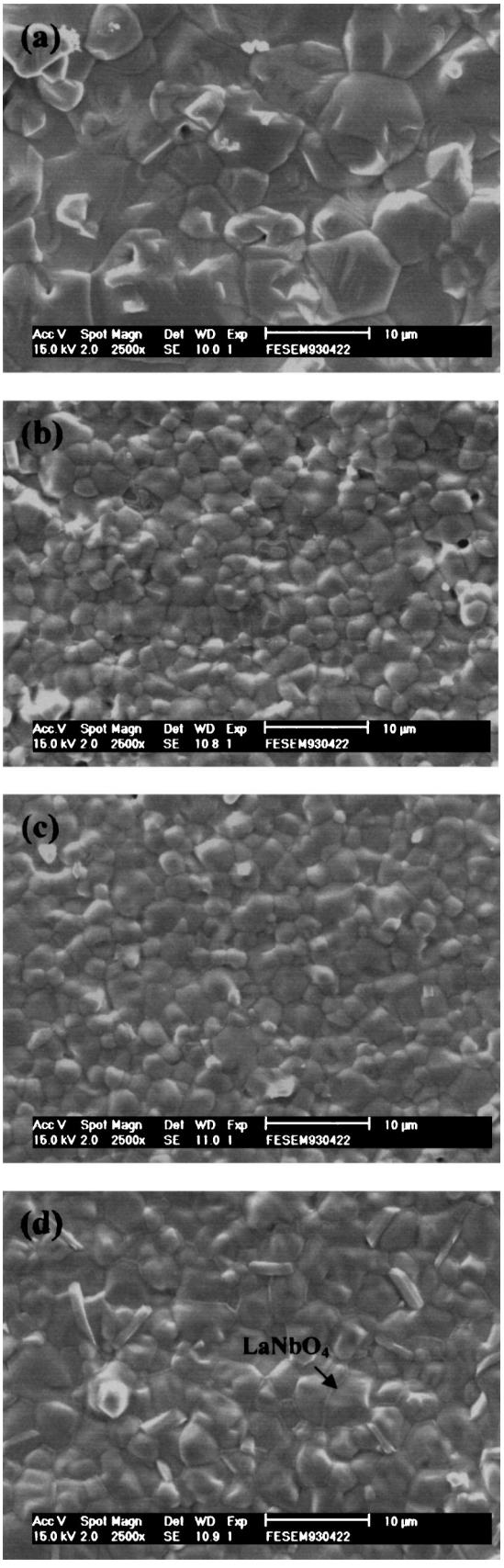

FIG. 4. SEM photographs of BFN sintered at 1350 °C for 4 h with a dopant of x% La_2O_3 (a) 2%, (b) 6%, (c) 8%, (d) and 20%.

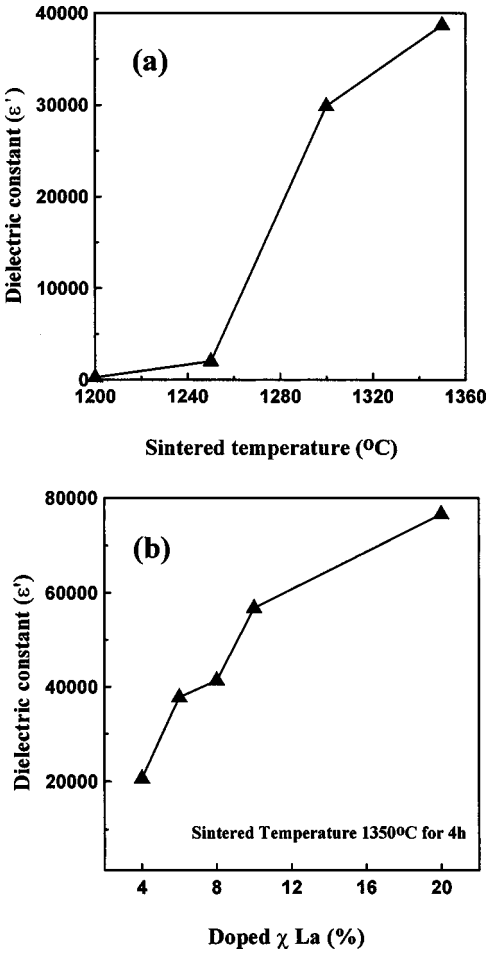

FIG. 5. (a) Dependence of dielectric constant with sintering temperature for 4% La-doped BFN and (b) The relationship of dielectric constant and doped level of x% La. Sintered at 1350 °C for 4 h.

The samples studied do not exhibit any ferroelectricity-related properties,[9] for example, the temperature dependence of the dielectric permittivity is not given by the Curie-Weiss law. Experimental evidence of electrical inhomogeneities in the samples suggests extrinsic effects. In general, the interpretation of the dielectric constant at low frequencies could be clarified on the basis of the interfacial polarization model.[15] Since Fe presents di- and trivalent ions simultaneously in oxide ceramics, two different compositions with the following formulas are considered in this case:

$$Ba_{1-x}^{2+}La_x^{3+}(Fe^{3+}Nb^{5+})_{1-\frac{x}{4}}O_3^{2-}, \tag{1}$$

$$Ba_{1-x}^{2+}La_x^{3+}(Fe^{2+}Nb^{5+})_{1-\frac{x}{4}}O_3^{2-}\square_{\frac{1}{2}-\frac{x}{8}}. \tag{2}$$

Charge compensation is provided by the oxygen vacancies shown by the open square. Assuming that the ceramics comprise grains consisting of formula (1) and grain boundaries consisting of formula (2). This is because the oxygen diffusion coefficient at the grain boundaries is much larger than in the bulk during the sintering process. Therefore, the extent of oxidation and subsequent resistivity are higher in the grain-boundary layers than in the grain. This fact, taken with the relatively small total width of the grain boundaries in the direction of the field, explains such large values of dielectric permittivity in the ceramics of interest.

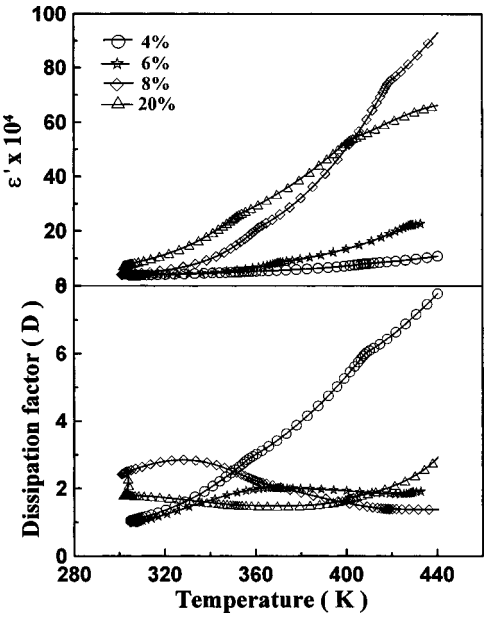

FIG. 6. Temperature dependence of ε'(upper curves) and loss tangent (lower curve) measured at 1 kHz for $Ba_{1-x}La_x(Fe_{0.5}Nb_{0.5})_{1-4/x}O_3$.

IV. CONCLUSION

When the La concentration increases, $Ba(FeNb)_{1/2}O_3$ exhibits a giant dielectric constant ($\varepsilon \sim 10^4-10^5$), as measured at 1 kHz. When La dopes $Ba(FeNb)_{1/2}O_3$ to over 20 mol%, a second phase $LaNbO_4$ is generated, as was revealed by the x-ray patterns. Because of the production of the secondary phase, this will cause the dielectric constant to drop. In the experiments, the electric and *B*-site vacancy compensations are predominantly in the undoped BFN at a low doping level. At high doping concentrations, either a self-compensation or a *B*-site vacancy compensation becomes more effective at the expense of electron compensation. Different compensation mechanisms apply at different La concentrations. A ceramic doped with an 8 mol% La concentration has a high static dielectric constant that rises from 4×10^4 to 8×10^5 as the temperature is increased from room temperature to 440 K. The present dielectric behavior was interpreted on the basis of the interfacial polarization at the grain-boundary region.

ACKNOWLEDGMENT

The authors would like to thank the National Science Council of the Republic of China for financially supporting this research under Contract No. NSC92-2216-E-006-026.

[1]C. C. Homes, T. Vogt, and S. M. Shaprio, Phys. Rev. B **67**, 092106 (2003).
[2]M. A. Subramanian, D. Li, N. Duan, B. A. Reisner, and A. W. Sleight, J. Solid State Chem. **151**, 323 (2000).
[3]J. Wu, C.-W. Nan, Y. Lin, and Y. Deng, Phys. Rev. Lett. **89**, 217601 (2002).
[4]S. Saha and T. P. Sinha, J. Phys.: Condens. Matter **14**, 249 (2002).
[5]W. Z. Zhu, A. Kholkin, P. Q. Mantas, and J. L. Baptista, J. Mater. Sci. **36**,

4098 (2001).
[6]W. Z. Zhu, A. Kholkin, P. Q. Mantas, and J. L. Baptista, J. Mater. Sci. **36**, 3447 (2001).
[7]F. D. Morrison, D. C. Sinclair, and A. R. West, J. Appl. Phys. **86**, 6355 (1999).
[8]F. D. Morrison, D. C. Sinclair, and A. R. West, Int. J. Inorg. Mater. **3**, 1205 (2001).
[9]I. P. Raevski, S. A. Prosandeev, A. S. Bogatin, M. A. Malitskaya, and L. Jastrabik, J. Appl. Phys. **93**, 4130 (2003).
[10]M. Mohsen, R. Krause-Rehberg, A. M. Massoud, and H. T. Langhammer, Radiat. Phys. Chem. **68**, 549 (2003).
[11]G. V. Lewis and C. R. A. Catlow, J. Phys. Chem. **47**, 89 (1986).
[12]C. Macchi, A. Somoza, A. Dupasquier, A. Lopez, and M. Castro, J. Phys.: Condens. Matter **13**, 5717 (2001).
[13]N. S. Hari and T. R. N. Kutty, J. Mater. Sci. **33**, 3275 (1998).
[14]N. H. Chan, R. K. Sharma, and D. M. Smyth, J. Am. Ceram. Soc. **65**, 167 (1984).
[15]M. Yokosuka, Jpn. J. Phys. **34**, 5338 (1995).